Transient Response Analysis of a Dispersive Periodic Grating After Deformation

Ryosuke Ozaki and Tsuneki Yamasaki

Abstract – Recently, we analyzed the issue of transient scattering for a slanted grating structure with an air region in a dispersive medium by combining the fast inverse Laplace transform method, Fourier series expansion method, and multilayer division method. In addition, we examined the influence of a slanted cavity from the resulting waveform on reflected electric and magnetic fields. In this article, we investigate the dispersive periodic grating after deformation. Consequently, we clarify the characteristics of the deformed cavity from the differential waveform of the reflected electric field.

1. Introduction

The transient scattering problem of electromagnetic waves is of interest in many engineering applications, including radar technology, such as shape recognition obtained from time response analysis. Recently, it has been applied in remote sensing and the further development of imaging technology. However, its application becomes significantly challenging in scenarios such as large-scale heavy rains caused by the deterioration of the global warming phenomenon worldwide. In Japan, the deterioration of infrastructure, such as roads or tunnels during periods of high economic growth, has become a social problem. The damage to buried pipes in the subsurface or the formation of cavities due to the seepage of rainwater underground can be considered one of the reasons for deterioration of roads or tunnels. Due to the above-mentioned reason, for example, the various shapes of cavities are formed by the state of the underground structure. Thus, it is necessary to monitor or regularly inspect the subsurface structure. In particular, ground-penetrating radar [1, 2] is handy in exploring the target objects in the subsurface structures. In this way, to express the underground structure with heterogeneous and complicated cavities, the subsurface structure is modeled by a periodic structure in our research.

This study aims to obtain the characteristics of a deformed cavity composed of a slanted grating structure. Consequently, we analyzed the transient response for slanted grating with the deformed cavity by combining the fast inverse Laplace transform (FILT) [3], Fourier series expansion method [4], and multilayer division methods [5, 6] and investigate the influence of the deformed cavity on the resulting waveform obtained from time response analysis.

2. Method of Analysis

We consider the structure for dispersive periodic grating after deformation and reflective plate embedded at $x = d_0$ as shown in Figure 1. $S_1(x \le 0)$ is free space with a dielectric constant ε_0. In $S_2(0 < x \le d_0)$, the dispersive medium $\varepsilon(s)$ and deformed cavity ε_0 are arranged in a periodic grating structure of period length p. Figure 1 is periodic in the y-direction and uniform in the z-direction. Here, the width of the slanted region is w, the slanted angle θ is defined as $\tan^{-1}(\delta/d_0)$, and δ is a parameter of the slanted width. The permeability in all the regions is assumed to be μ_0. The time factor of the electromagnetic fields is assumed to be $\exp(st)$ in the complex frequency domain and is suppressed in this study.

The TE (the electric field has only the z-component) case is discussed in the following formulation. The electromagnetic field in the complex frequency domain is expressed as "^" and distinguished from those in the time domain. The waveform of the incident pulse at $x = 0$ is assumed to be a sine pulse in the time domain, and its image function can be expressed as follows:

$$\widehat{E}_0^{(i)} = \frac{\omega_0}{s^2 + \omega_0^2}\left(1 - e^{-st_w}\right) \tag{1}$$

where $\omega_0(:= 2\pi/t_w)$ is angular frequency, s is the complex frequency, $t_w(:= 1/f_0)$ is the pulse width, and f_0 is center frequency. When the sine pulse is assumed to be a normal incidence from $x \le 0$, the electric field in S_1 is expressed as follows:

$$\widehat{E}_z^{(1)}(x, y) = \widehat{E}_z^{(i)}(x) + \widehat{E}_z^{(r)}(x, y) \tag{2}$$

where the incident electric field $\widehat{E}_z^{(i)}(x)$ and reflected electric field $\widehat{E}_z^{(r)}(x, y)$ are expressed as follows:

$$\widehat{E}_z^{(i)}(x) = \widehat{E}_0^{(i)} e^{-\hat{k}_0 x} \tag{3}$$

$$\widehat{E}_z^{(r)}(x, y) = \sum_{n=-N_1}^{N_1} R_n e^{\widehat{k_1^{(n)}} x - i\frac{2n\pi}{p} y} \tag{4}$$

$$\widehat{k}_1^{(n)} := \sqrt{\widehat{k}_0^2 - (-i2n\pi/p)^2},\ \widehat{k}_0 := s/c_0 \tag{5}$$

where N_1 is the truncation mode number of the electromagnetic field, $\widehat{k}_0$ is the wave number in free

Manuscript received 20 September 2022.

Ryosuke Ozaki and Tsuneki Yamasaki are with the Department of Electrical Engineering, College of Science and Technology, Nihon University, 1-8-14 Surugadai, Kanda, Chiyoda-ku, Tokyo 101-8308, Japan; e-mail: ozaki.ryousuke@nihon-u.ac.jp, yamasaki.tsuneki@nihon-u.ac.jp.

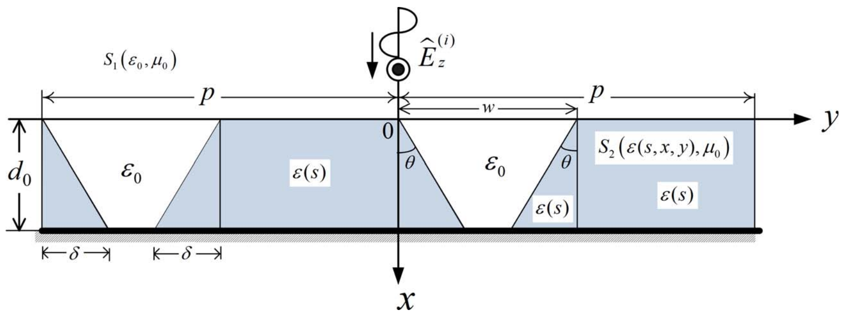

Figure 1. Structure of the dispersive medium with a deformed cavity.

space, c_0 is the velocity of light, and $\widehat{k}_1^{(n)}$ is the propagation constant in the x-direction.

In the region S_2, the electromagnetic field can be expressed by applying the multilayer division method, as shown in Figure 2. The region S_2 is divided into M thin slanted layers, and the permittivity distribution $\varepsilon(s,x,y)$ in each layer is approximated using a step-index profile in the y-direction. To determine the electromagnetic fields in each thin layer, we expand the electromagnetic fields using eigenvalues $h_v^{(l)}$ and eigenvectors $u_{v,n}^{(l)}$ obtained from the eigenvalue equation [5] as follows:

$$\widehat{E}_z^{(2,l)}(x,y) = \sum_{v=1}^{2N_1+1} [\alpha_v^{(l)} + \beta_v^{(l)}] \sum_{n=-N_1}^{N_1} u_{v,n}^{(l)} e^{-i\frac{2n\pi}{p}y} \quad (6)$$

$$\alpha_v^{(l)} := A_v^{(l)} e^{-h_v^{(l)}\{x-(l-1)d_m\}}, \beta_v^{(l)} := B_v^{(l)} e^{h_v^{(l)}\{x-ld_m\}} \quad (7)$$

$$d_m := d_0/M, 1 \le l \le M,$$

$$\widehat{H}_y^{(j)}(x,y) := \frac{1}{\mu_0 s}\frac{\partial \widehat{E}_z^{(j)}(x,y)}{\partial x}, (j=1,2) \quad (8)$$

where the superscript l indicates the lth layer and $A_v^{(l)}$,$B_v^{(l)}$ are unknown coefficients to be determined from the boundary conditions. In the previously mentioned electromagnetic fields, we derived the relational expression of the unknown coefficients from boundary conditions at $x=0$, $x=d_0$ and $x=ld_m$ $(l=1\sim(M-1))$.

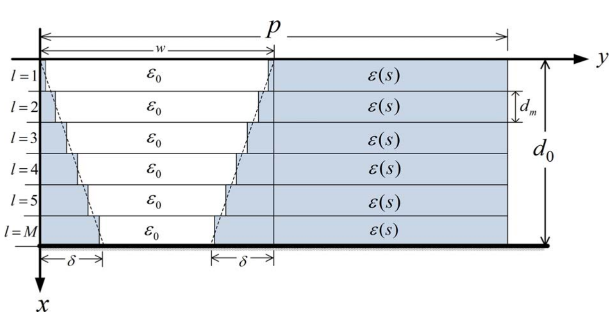

Figure 2. Example of the approximated multilayer division method for a deformed region.

First, the following equations can be obtained by matrix algebra from the boundary conditions at $x=0$ and $x=d_0$:

$$\mathbf{Q}_1\mathbf{A}^{(1)} + \mathbf{Q}_2\mathbf{B}^{(1)} = \mathbf{E}_i \quad (9)$$

$$\mathbf{Q}_3\mathbf{A}^{(M)} + \mathbf{Q}_4\mathbf{B}^{(M)} = 0 \quad (10)$$

where

$$\mathbf{Q}_\kappa := [q_{v,n}^{(\kappa)}], \kappa = 1\sim 4,$$

$$q_{v,n}^{(1)} := (\widehat{k}_1^{(n)} + h_v^{(1)})u_{v,n}^{(1)}, q_{v,n}^{(2)} := (\widehat{k}_1^{(n)} - h_v^{(1)})u_{v,n}^{(1)}e^{-h_v^{(1)}d_m},$$

$$q_{v,n}^{(3)} := e^{-h_v^{(M)}d_m}u_{v,n}^{(M)}, q_{v,n}^{(4)} := u_{v,n}^{(M)},$$

$$v = 1\sim(2N_1+1), -N_1 \le n \le N_1,$$

$$\mathbf{A}^{(\imath)} := [A_1^{(\imath)}, A_2^{(\imath)}, \cdots, A_{2N_1+1}^{(\imath)}]^T,$$

$$\mathbf{B}^{(\imath)} := [B_1^{(\imath)}, B_2^{(\imath)}, \cdots, B_{2N_1+1}^{(\imath)}]^T, \imath = 1 \text{ or } M,$$

$$\mathbf{E}_i := [0,\cdots,(k_0+k_1^{(n)})E_0^{(i)},\cdots,0]^T, T = \text{transpose}.$$

Using the boundary condition at $x=ld_m$, the following matrix relation between $\mathbf{A}^{(1)}, \mathbf{B}^{(1)}$ and $\mathbf{A}^{(M)}$, $\mathbf{B}^{(M)}$ can be obtained:

$$\begin{pmatrix}\mathbf{A}^{(1)}\\ \mathbf{B}^{(1)}\end{pmatrix} = \begin{pmatrix}\mathbf{G}_1^{(1)} & \mathbf{G}_2^{(1)}\\ \mathbf{G}_3^{(1)} & \mathbf{G}_4^{(1)}\end{pmatrix}\cdots\begin{pmatrix}\mathbf{G}_1^{(M-1)} & \mathbf{G}_2^{(M-1)}\\ \mathbf{G}_3^{(M-1)} & \mathbf{G}_4^{(M-1)}\end{pmatrix}\begin{pmatrix}\mathbf{A}^{(M)}\\ \mathbf{B}^{(M)}\end{pmatrix},$$

$$= \begin{pmatrix}\mathbf{G}_1 & \mathbf{G}_2\\ \mathbf{G}_3 & \mathbf{G}_4\end{pmatrix}\begin{pmatrix}\mathbf{A}^{(M)}\\ \mathbf{B}^{(M)}\end{pmatrix} \quad (11)$$

where

$$\mathbf{G}_\kappa^{(l)} := [g_{v,n}^{(\kappa,l)}], \kappa = 1\sim 4, l = 1\sim(M-1),$$

$$g_{v,n}^{(1,l)} := \left[\Gamma_{v,n}^{(l)} + \Gamma_{v,n}^{(l)} h_v^{(l+1)} \Big/ h_v^{(l)}\right] e^{h_v^{(l)}d_m} \Big/ 2,$$

$$g_{v,n}^{(2,l)} := \left[\Gamma_{v,n}^{(l)} - \Gamma_{v,n}^{(l)} h_v^{(l+1)} \Big/ h_v^{(l)}\right] e^{-(h_v^{(l+1)} - h_v^{(l)}) d_m} \Big/ 2,$$

$$g_{v,n}^{(3,l)} := \left[\Gamma_{v,n}^{(l)} - \Gamma_{v,n}^{(l)} h_v^{(l+1)} \Big/ h_v^{(l)}\right] \Big/ 2,$$

$$g_{v,n}^{(4,l)} := \left[\Gamma_{v,n}^{(l)} + \Gamma_{v,n}^{(l)} h_v^{(l+1)} \Big/ h_v^{(l)}\right] e^{-h_v^{(l+1)} d_m} \Big/ 2,$$

$$\Gamma_{v,n}^{(l)} := [u_{v,n}^{(l)}]^{-1} \cdot [u_{v,n}^{(l+1)}],$$

$$v = 1 \sim (2N_1 + 1), -N_1 \leq n \leq N_1$$

Eliminating $\mathbf{A}^{(1)}$, $\mathbf{B}^{(1)}$, and $\mathbf{B}^{(M)}$ from (9)–(11), the following matrix simultaneous equation is obtained:

$$\mathbf{X}_t \cdot \mathbf{A}^{(M)} = \mathbf{E}_i \tag{12}$$

where

$$\mathbf{X}_t := [(\mathbf{Q}_1\mathbf{G}_1 + \mathbf{Q}_2\mathbf{G}_3) - (\mathbf{Q}_1\mathbf{G}_2 + \mathbf{Q}_2\mathbf{G}_4)\mathbf{Q}_4^{-1}\mathbf{Q}_3].$$

We determine the other unknown coefficients $\mathbf{A}^{(1)}$, $\mathbf{B}^{(1)}$, and $\mathbf{B}^{(M)}$ by solving (12). Therefore, we evaluated the reflection coefficients R_n using the unknown coefficients. The reflected electric field $E_z^{(r)}(x, y)$ in the complex frequency domain obtained from (4) is transformed into the normalized time domain by utilizing the following FILT method [3]:

$$E_z^{(r)}(T) = \frac{1}{2\pi i} \int_{\gamma - i\infty}^{\gamma + i\infty} E_z^{(r)}(S, X, Y) e^{ST} dS,$$

$$= \frac{e^a}{T} \left[\sum_{n=1}^{N} F_n + 2^{-J} \sum_{L=1}^{J} C_{JL} F_{N+L}\right] \tag{13}$$

where

$$F_n = (-1)^n \mathrm{Im}\left[\widehat{E}_z^{(r)}(X, Y)\right], S := \frac{a + i(n - 0.5)\pi}{T},$$

$$C_{JJ} = 1, C_{JL-1} := C_{JL} + \frac{J!}{(L-1)!(J-L-1)!}$$

Here, N is the truncation mode number of the FILT method, J is the number of terms in the Euler transformation, $S(:= st_w)$ is the normalized complex frequency, $T(:= t/t_w)$ is the normalized time, and $X(:= x/d_0)$ and $Y(:= y/p)$ are the normalized coordinates.

3. Numerical Results

The values of the chosen parameters were $f_0 = 1\text{GHz}$, normalized period $P(:= p/(t_w c_0)) = 1$, normalized depth $D_0(:= d_0/p) = 0.2$, and normalized width of slanted region $W_p(:= w/p) = 0.5$. Thus, the dispersive medium is expressed using the parameters (g_m, ξ_m, Θ_m, τ_0, τ) with 5% soil moisture $\varepsilon(s)$ [7] as follows:

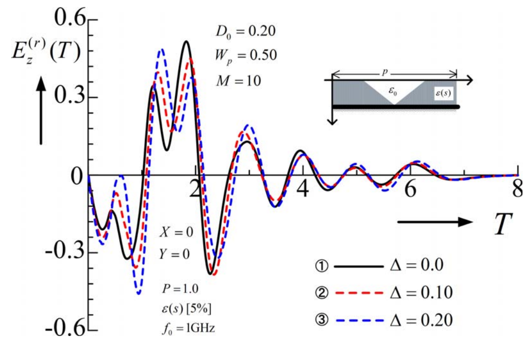

Figure 3. Waveform of time response by varying the slanted width Δ.

$$\frac{\varepsilon(s)}{\varepsilon_0} = 1 + \sum_{m=1}^{3} \frac{\Theta_m^2}{s^2 + g_m s + \xi_m^2} + \frac{\tau}{1 + s\tau_0} \tag{14}$$

For all the results, the calculation parameters are fixed as $N_1 = 20$, $M = 10$, $a = 4$, $N = 10$, $J = 5$, and $X = 0$, $Y = 0$.

The time response waveform for the reflected electric field $E_z^{(r)}(T)$ obtained by varying the normalized slanted width $\Delta(:= \delta/d_0)$ is shown in Figure 3, where the effect of Δ is seen at $0.5 < T < 2.0$ as Δ increase. From the figure, ①$\Delta = 0.0$, ②$\Delta = 0.1$, and ③$\Delta = 0.2$. This effect is almost similar to the case with the previous slanted air region [4, 5]. We examined the differential waveform based on the results obtained from Figure 3 to validate this effect.

The differential waveform $f_z^{(r)}(T)$ obtained using the results of ①, ②, and ③ in Figure 3 is shown in Figure 4. The following features can be observed in Figure 4:

(1-1) The phase of both the results was almost the same. However, a phase difference was observed from approximately $T = 2.5$.

(1-2) The shape of the deformed cavity can be identified from the response amplitude using only the reflected electric field. This point differs from the influence in the case of a previous slanted cavity [4, 5].

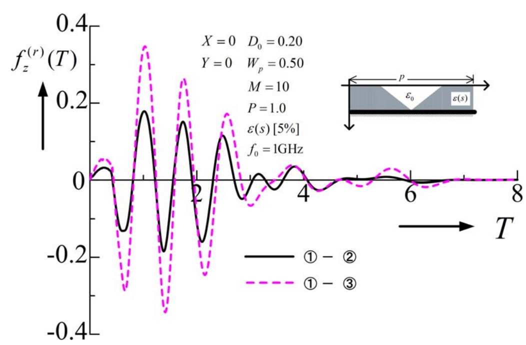

Figure 4. Differential waveform in Figure 3.

4. Conclusions

This study investigated the transient response analysis for a dispersive periodic grating after deformation using the combination of FILT, Fourier series expansion, and multilayer division methods. In addition, we investigated the influence of the deformed cavity on resulting waveforms. Consequently, we obtained the characteristics of the deformed symmetric cavity from the differential waveform of the reflected electric field.

The influence of an arbitrary cavity shape that comprises a slanted structure will be investigated in the future.

5. Acknowledgment

This study was partially supported by JSPS KAKENHI grant number JP21K04239.

6. References

1. R. Persico, *Introduction to Ground Penetrating Radar Inverse Scattering and Data Processing*, New York, Wiley, 2013.
2. P. Shannuan and I. L. Al-Qadi, "Calibration of FDTD Simulation of GPR Signal for Asphalt Pavement Compaction Monitoring," *IEEE Transactions on Geoscience and Remote Sensing*, **53**, 3, 2015, pp. 1538-1548.
3. T. Hosono, "Numerical Inversion of Laplace Transform and Some Applications to Wave Optics," *Radio Science*, **16**, 6, 1981, pp. 1015-1019.
4. R. Ozaki and T. Yamasaki, "Pulse Responses From Periodically Arrayed Dispersion Media With an Air Region," *IEICE Transactions on Electronics*, **E102-C**, 6, 2019, pp. 479-486.
5. R. Ozaki and T. Yamasaki, "Numerical Analysis of Pulse Response for Slanted Grating Structure With an Air Region in Dispersion Media by TE Case," *IEICE Transactions on Electronics*, **E105-C**, 4, 2022, pp. 154-158.
6. R. Ozaki and T. Yamasaki, "Transient Response for Slanted Gratings in Dispersion Medium," 3rd URSI Atlantic Radio Science Meeting, Gran Canaria, Spain, May 29–June 3, 2022.
7. R. Ozaki, N. Sugizaki, and T. Yamasaki, "Numerical Analysis of Pulse Response in the Dispersion Media," *IEICE Transactions on Electronics*, **E97-C**, 1, 2014, pp. 45-49.